Highly Anisotropic Exchange Interactions in a Trigonal Bipyramidal Cyanide-Bridged $Ni^{II}_3Os^{III}_2$ Cluster

Andrei V. Palii,*,† Oleg S. Reu,† Sergei M. Ostrovsky,† Sophia I. Klokishner,† Boris S. Tsukerblat,*,‡ Matthew Hilfiger,§ Michael Shatruk,|| Andrey Prosvirin,§ and Kim R. Dunbar*,§

Institute of Applied Physics of the Academy of Sciences of Moldova, Academy str. 5, Chisinau MD-2068, Moldova, Chemistry Department, Ben-Gurion University of the Negev, Beer-Sheva 84105, Israel, Department of Chemistry, Texas A&M University, P.O. Box 30012, College Station, Texas 77843-3012, and Department of Chemistry and Biochemistry, Florida State University, Tallahassee, Florida 32306

Received: March 11, 2009; Revised Manuscript Received: May 1, 2009

This article is a part of our efforts to control the magnetic anisotropy in cyanide-based exchange-coupled systems with the eventual goal to obtain single-molecule magnets with higher blocking temperatures. We give the theoretical interpretation of the magnetic properties of the new pentanuclear complex $\{[Ni^{II}(tmphen)_2]_3[Os^{III}(CN)_6]_2\}\cdot 6CH_3CN$ ($Ni^{II}_3Os^{III}_2$ cluster). Because the system contains the heavy Os^{III} ions, spin−orbit coupling considerably exceeds the contributions from the low-symmetry crystal field and exchange coupling. The magnetic properties of the $Ni^{II}_3Os^{III}_2$ cluster are described in the framework of a highly anisotropic pseudo-spin Hamiltonian that corresponds to the limit of strong spin−orbital coupling and takes into account the complex molecular structure. The model provides a good fit to the experimental data and allows the conclusion that the trigonal axis of the bipyramidal $Ni^{II}_3Os^{III}_2$ cluster is a hard axis of magnetization. This explains the fact that in contrast with the isostructural trigonal bipyramidal $Mn^{III}_2Mn^{II}_3$ cluster, the $Ni^{II}_3Os^{III}_2$ system does not exhibit the single-molecule magnetic behavior.

1. Introduction

Over a decade ago, it was understood that the negative zero-field splitting of the ground state $S = 10$ of the so-called Mn_{12} cluster, $Mn_{12}O_{12}(CH_3COO)_{16}\cdot 4H_2O$, gives rise to a slow magnetic relaxation that is a signature of single molecule magnetism.[1,2] The barrier for spin reorientation in single molecule magnets (SMMs) is a key characteristic for this kind of system, and many attempts have been undertaken to increase the barrier and, consequently, the relaxation time.

A general idea for essentially increasing the magnetic barrier by exploiting strongly anisotropic unquenched orbital contributions has been discussed in the context of the broader problem of orbital degeneracy in magnetic exchange,[3−9] considering, in particular, the role of spin−orbital coupling.[8,10,11] In striving to implement this concept, we have turned to the cyanide clusters,[8,9,12−17] whose structural motifs contain metal ions in nearly perfect octahedral sites, a situation that leads to orbital degeneracy. A relatively high degree of synthetic control available in cyanide coordination chemistry allows for the variation of the metal ions and their positions in a heterometallic cyanide-bridged cluster and makes it feasible to design systems with controllable parameters. The degree of the anisotropy was shown to depend on the interrelation between spin−orbital interaction, strength (and sign) of the low symmetric component of the crystal field, and exchange interactions.[8,9]

Recently, one of our groups reported the synthesis and magnetic properties of the new pentanuclear complex $\{[Ni^{II}(tmphen)_2]_3[Os^{III}(CN)_6]_2\}\cdot 6CH_3CN$ ($Ni^{II}_3Os^{III}_2$ cluster).[18] The magnetic data in our original report[18] were interpreted by means of a simple spin-only model that resulted in an unrealistically large zero-field splitting parameter, D. From a general point of view, the spin model of exchange seems to be inapplicable to the orbitally degenerate ions, such as Os(III) in an octahedral crystal field. Consequently, we propose here a more realistic approach within which we go beyond the spin model to provide an adequate explanation of the observed magnetic behavior of the $Ni^{II}_3Os^{III}_2$ cluster. In terms of magnetic anisotropy, the heavier transition-metal clusters based on orbitally degenerate ions exhibit strong spin−orbit coupling, which considerably exceeds the contributions from the low-symmetry crystal field and exchange coupling. The aim of this article is to describe the magnetic properties of the $Ni^{II}_3Os^{III}_2$ cluster in the framework of a highly anisotropic pseudo-spin Hamiltonian that takes into account strong spin−orbit coupling and the complex molecular structure of the title compound.

2. Pseudo-Spin Hamiltonian for the $Ni^{II}_3Os^{III}_2$ Cluster

The crystal structure analysis revealed that the $Ni^{II}_3Os^{III}_2$ cluster consists of two axial $[Os(CN)_6]^{3-}$ units connected via bridging cyanide ligands to three equatorial $[Ni(tmphen)_2]^{2+}$ moieties to yield a trigonal bipyramidal geometry (Figure 1). As relevant to our analysis of the magnetic anisotropy of Os(III) centers presented herein, we note that the Os−CN bond lengths and CN−Os−CN bond angles obviously show nearly octahedral symmetry of the $[Os(CN)_6]^{3-}$ fragments with a slight distortion. (See the Appendix.) These fragments are not crystallographically equivalent, but the inspection of their coordination geometry shows that Os(III) centers are very similar and can be described with one set of magnetic parameters to avoid overparametrization. The

* Corresponding authors. E-mail: andrew.palii@uv.es (A.V.P.); tsuker@bgu.ac.il (B.S.T.); dunbar@mail.chem.tamu.edu (K.R.D.).
† Institute of Applied Physics of the Academy of Sciences of Moldova.
‡ Ben-Gurion University of the Negev.
§ Texas A&M University.
|| Florida State University.

10.1021/jp902197n CCC: $40.75
Published on Web 06/04/2009

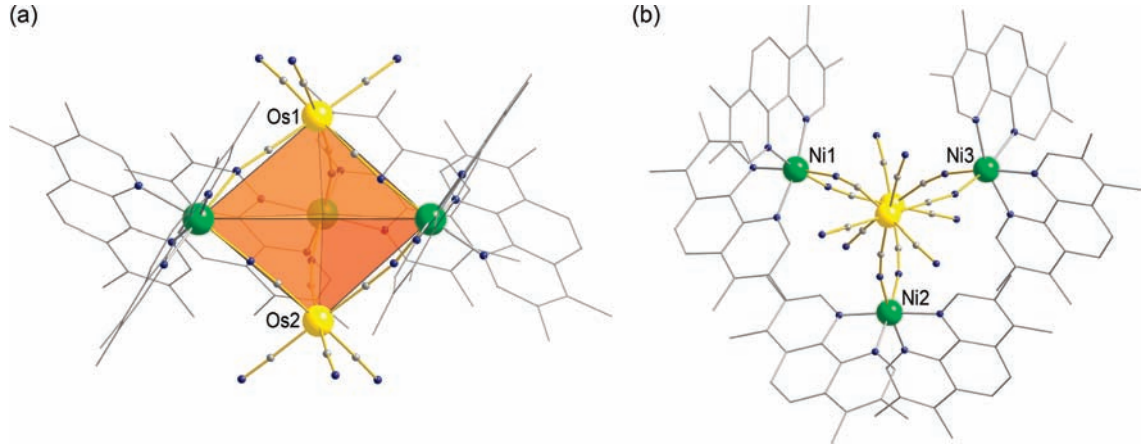

Figure 1. Molecular structure of the Ni_3Os_2 complex in which metal ions are in the Ni^{II} and Os^{III} states: (a) Side view emphasizing the NiN_6 and OsC_6 coordination environments; the trigonal bipyramidal cluster core is highlighted with a hypothetical polyhedron. (b) View along the axis of the trigonal bipyramid emphasizing the approximately trigonal symmetry around each Os site. To allow for a better view of the cluster core, the tmphen ligands are shown in the stick mode, and the H atoms are omitted. Color scheme: Ni = green, Os = yellow, N = blue, C = gray.

assumption about idealized D_{3h} geometry will be used in the formulation of the exchange model throughout this work.

The magnetic properties of this compound were previously modeled by one of us,[18] taking into account the intracluster isotropic superexchange (Heisenberg−Dirac−Van Vleck model, HDVV) and the zero-field splitting for the Ni(II) ions (with the isotropic Zeeman interaction)

$$H = -2J_{\mathrm{Ni-Os}}(\mathbf{s}_{\mathrm{Os1}} + \mathbf{s}_{\mathrm{Os2}})(\mathbf{s}_{\mathrm{Ni1}} + \mathbf{s}_{\mathrm{Ni2}} + \mathbf{s}_{\mathrm{Ni3}}) - D_{\mathrm{Ni}} \sum_{k=1,2,3} [s^2_{\mathrm{ZNi}k} - s_{\mathrm{Ni}}(s_{\mathrm{Ni}} + 1)/3] \quad (1)$$

Application of this Hamiltonian resulted in the best fit parameters $J_{\mathrm{Ni-Os}} = 2.3\ \mathrm{cm}^{-1}$ and $D_{\mathrm{Ni}} = 19.5\ \mathrm{cm}^{-1}$ ($g = 2.09$). As mentioned in ref 18, the D parameter is unrealistically large for the Ni(II) ion. From a general point of view, the spin model of exchange seems to be inapplicable to the orbitally degenerate ions such as Os(III) in an octahedral crystal field. This conclusion shows that the spin model is unable to give an adequate description of the magnetic properties of the title compound, and a more sophisticated approach is required.

The ground state of the Ni(II) ion in the octahedral surrounding of the N-bound cyanide ligands is the orbital singlet $^3A_2(t_2^6e^2)$. A strong cubic crystal field induced by six C-bound cyanides gives rise to the triply degenerate ground term $^2T_2(t_2^5)$ for the Os(III) ion. Under the condition of orbital degeneracy, the HDVV model (eq 1) is inapplicable even as an approximation, and the problem of the magnetic exchange was shown to be much more complicated.[3,4] Here we will employ a model that explicitly takes into account strong spin−orbital interaction in the $^2T_2(t_2^5)$ term for the Os(III) ion. The spin−orbit interaction splits this term into the Kramers doublet Γ_7 and quadruplet Γ_8 (we use the conventional Bethe's notations for the double-valued irreducible representations), with the doublet $\Gamma_7(\pm 1/2)$ (effective spin 1/2) being the ground state. Because the energy gap between the Γ_7 and Γ_8 levels for the osmium ions exceeds 5000 cm^{-1},[19] the group of the low-lying energy levels of the system, in which only the Γ_7 doublet of the Os(III) ion is involved in exchange interactions, is well separated from the remaining part of the energy spectrum. In this case, the exchange Hamiltonian describing the low-lying levels includes pseudo-spin-1/2 operators related to two Os(III) ions and true spin-1 operators related to three Ni(II) ions, for which the orbital contribution is very small. This Hamiltonian is expected to provide good accuracy in the description of the magnetic data for the $Ni^{II}_3Os^{III}_2$ cluster up to room temperature.

The effective g factor for the Kramers doublet $\Gamma_7(\pm 1/2)$ of the Os(III) ion in a perfect octahedral ligand field is found to be

$$g_{\mathrm{eff}}(\mathrm{Os}) = (g_e + 4\kappa)/3 \quad (2)$$

where g_e is the electronic g factor and κ is the orbital reduction factor. In further calculations, we will use the value of $\kappa = 0.66$ obtained by fitting the magnetic data and electronic absorption spectra for the free $[Os(CN)_6]^{3-}$ anion.[19] Substituting this value of κ into eq 2, we obtain $g_{\mathrm{eff}}(\mathrm{Os}) = 1.55$ that will be used in the subsequent calculations of the magnetic susceptibility data for the $Ni^{II}_3Os^{III}_2$ cluster. To avoid overparameterization, we do not take into account the zero-field splitting of the spin levels of Ni(II) ions and the anisotropy of the g factor for Ni(II) ions (local factors of the anisotropy). We assume a typical value of $g(\mathrm{Ni}) = 2.2$.[20] In this case, the Zeeman interaction becomes isotropic; therefore, the source of the magnetic anisotropy in the system can be related solely to the exchange interactions.

As follows from the general consideration of the orbital degeneracy in magnetic exchange,[6,7] the effective exchange interaction between Os(III) and Ni(II) ions is highly anisotropic because of orbitally dependent contributions to the exchange Hamiltonian.[21] In developing the exchange Hamiltonian for the $Ni^{II}_3Os^{III}_2$ cluster, we will use two kinds of frames: (1) local frames associated with six different Os−Ni pairs to write down the exchange coupling for each pair and (2) a common molecular frame to describe the total Hamiltonian of the cluster. The numbering of the paramagnetic ions, the molecular frame XYZ, and one of the local frames, $X_{13}Y_{13}Z_{13}$, related to the Os(1)−Ni(3) pair are shown in Figure 2. On the basis of single-crystal X-ray data for the $Ni^{II}_3Os^{III}_2$ complex, one can simplify the subsequent analysis assuming an idealized D_{3h} symmetry of the cluster. This assumption treats the complex as a perfect trigonal bipyramid in which the Ni triad forms an equilateral triangle and the trigonal axis passes through the apical Os(1) and Os(2) ions. To simplify calculations, we also assume that each Os−CN−Ni fragment has a perfectly linear arrangement.

The molecular Z axis is chosen to coincide with the C_3 axis of the trigonal bipyramid, and the X axis is chosen to be directed from the center of the triangle formed by the three Ni ions

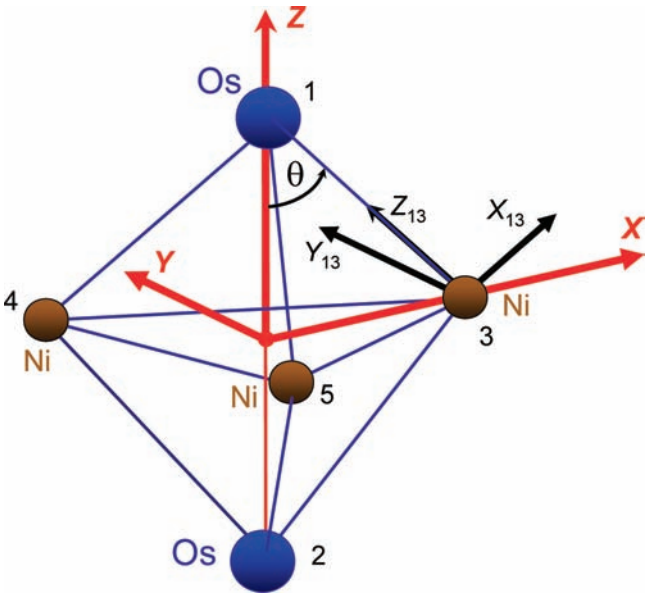

Figure 2. Metal skeleton of the $Ni_3^{II}Os^{III}_2$ cluster with the numbering of ions and the local and molecular frames.

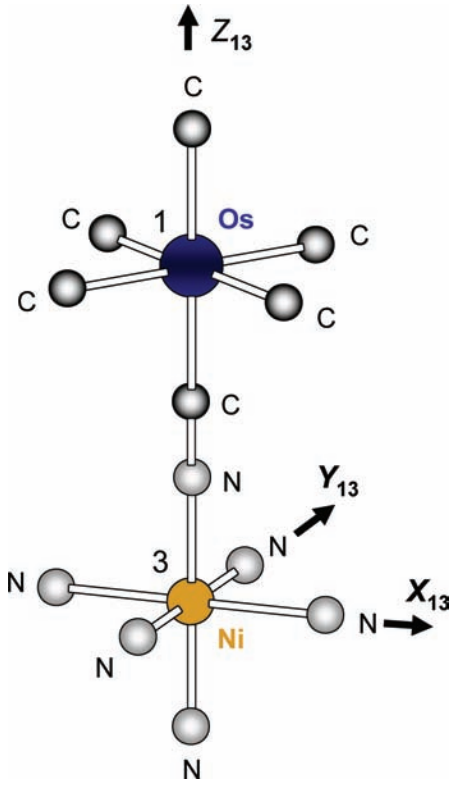

Figure 3. Local frame for $(NC)_5Os(\mu\text{-}CN)NiN_5$ bioctahedral fragment.

toward the Ni(3) ion. With this choice of the Z direction, the XY plane coincides with the equatorial plane formed by Ni ions. The local Z_{13} axis is directed along the Ni(3)−NC−Os(1) linear group. Within the adopted idealized geometry, the angle θ between the Z_{13} and Z axes is equal to 54.7°. The $X_{13}Z_{13}$ plane is chosen to coincide with the XZ plane, such that the Y_{13} axis is parallel to Y. In Figure 3, one can see that the local X_{13} and Y_{13} axes are directed from the Ni(3) ion toward the N atoms of its nearest ligand surroundings (tetragonal axes of the NiN_6 octahedron). The local $X_{14}Y_{14}Z_{14}$ and $X_{15}Y_{15}Z_{15}$ frames (not shown in Figure 2) are obtained from the $X_{13}Y_{13}Z_{13}$ frame through rotations around the Z axis by 120 and 240°, respectively. Finally, the local frames $X_{23}Y_{23}Z_{23}$, $X_{24}Y_{24}Z_{24}$, and $X_{25}Y_{25}Z_{25}$ are obtained from frames $X_{13}Y_{13}Z_{13}$, $X_{14}Y_{14}Z_{14}$, and $X_{15}Y_{15}Z_{15}$, respectively, through the reflections in the Ni_3 plane.

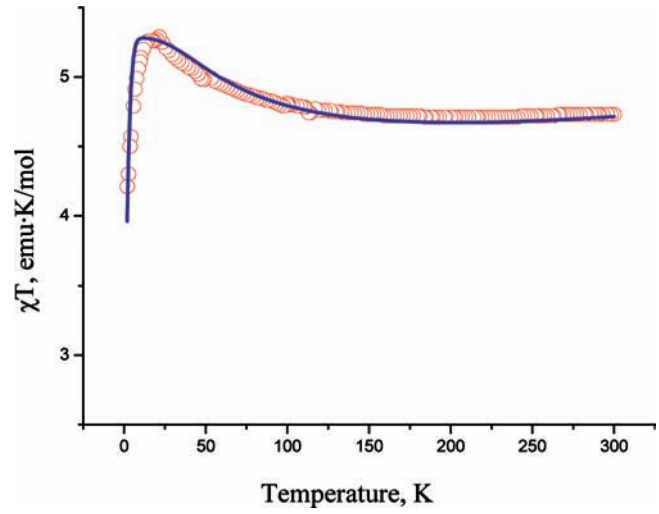

Figure 4. Comparison of the experimental (red circles) and theoretical (blue line) χT versus T curves for the powder sample of $Ni^{II}_3Os^{III}_2$. The theoretical curve was calculated with the best fit parameters $g_{eff}(Os) = 1.55$ and $g(Ni) = 2.2$. (See the text.)

Taking into account the tetragonal symmetry of the $(NC)_5Os(\mu\text{-}CN)NiN_5$ bioctahedron (Figure 3), we obtain the general form of the exchange Hamiltonian for the Os(1)−Ni(3) pair

$$H_{ex}(1,3) = -2J_{||}\tau_{Z_{13}}(1)s_{Z_{13}}(3) - 2J_{\perp}[\tau_{X_{13}}(1)s_{X_{13}}(3) + \tau_{Y_{13}}(1)s_{Y_{13}}(3)] \quad (3)$$

where $J_{||}$ and $J_{\perp}$ are the exchange parameters, $\tau_{Z_{13}}(1)$, $\tau_{X_{13}}(1)$, and $\tau_{Y_{13}}(1)$ are the components of the pseudo-spin-1/2 operator related to the ground Kramers doublet of the Os(III) ion, and $s_{Z_{13}}(3)$, $s_{X_{13}}(3)$, and $s_{Y_{13}}(3)$ represent the components of the true spin operators for the Ni(II) ion ($s_3 = 1$). All of these operators are defined in the local frame of the Os(1)−Ni(3) pair. Now, we pass from the operators defined in the local frames to the operators defined in the molecular frame. Omitting the details of these transformations, we arrive at the following total Hamiltonian of the $Ni^{II}_3Os^{III}_2$ cluster (including summation over all Os−Ni pairs) containing both exchange and isotropic Zeeman contributions

$$H_{ex} = -2\sum_{i=1,2}\sum_{j=3,4,5}\sum_{\alpha,\beta=X,Y,Z}\{J_{\alpha\beta}(i,j)\tau_{\alpha}(i)s_{\beta}(j) + \mu_B[g_{eff}(Os)\boldsymbol{\tau}_{12} + g(Ni)\mathbf{s}_{345}]\boldsymbol{H}\} \quad (4)$$

where $\boldsymbol{\tau}_{12} = \boldsymbol{\tau}_1 + \boldsymbol{\tau}_2$ is the pseudo-spin operator of the Os pair, $\mathbf{s}_{345} = \mathbf{s}_3 + \mathbf{s}_4 + \mathbf{s}_5$ is the spin operator of the Ni triad, and $\boldsymbol{H}$ is the magnetic field. The exchange parameters $J_{\alpha\beta}(i,j)$ are expressed in terms of the exchange integrals $J_{||}$, $J_{\perp}$, and the angle θ. (See the Appendix.)

3. Discussion of the Experimental Data

The experimental χT versus T data for the powder sample reported in ref 18 are shown in Figure 4 with red circles. It was observed that the $Ni^{II}_3Os^{III}_2$ cluster exhibits ferromagnetic coupling between the Ni(II) and Os(III) centers. A plot of χT versus T shows a slight increase as the temperature decreases, reaching a maximum of 5.29 emu·K/mol at 21.6 K; below this

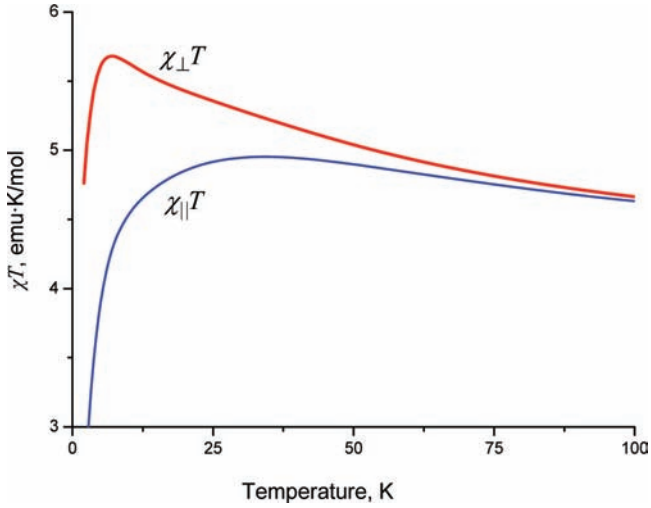

Figure 5. $\chi_{||}T$ versus T and $\chi_{\perp}T$ versus T curves calculated with g_{eff}(Os) = 1.55, g(Ni) = 2.2, $J_{||}$ = 23.8 cm^{-1}, and $J_{\perp}$ = 1.2 cm^{-1}. (TIP is not included.)

temperature, χT decreases abruptly upon cooling. One can see that the anisotropic exchange model allows us to reproduce all features of the temperature-dependent behavior of χT, with the best fit parameters $J_{||}$ = 23.8 cm^{-1}, $J_{\perp}$ = 1.2 cm^{-1}, χ_{TIP} = 1.4 × 10^{-3} cm^{-1}, and the R factor

$$R = \sqrt{\frac{1}{N}\sum_{i=1}^{N}\frac{[(\chi_i T_i)_{theor} - (\chi_i T_i)_{exptl}]^2}{(\chi_i T_i)^2_{exptl}}} = 1.54 \times 10^{-2} \quad (5)$$

Figure 5 depicts the temperature dependence of $\chi_{||}T$ and $\chi_{\perp}T$ calculated with the best-fit parameters. It can be seen that $\chi_{\perp} > \chi_{||}$, which means that the trigonal Z axis of the bipyramid is the hard axis of magnetization (or the Ni^{II}_3 plane is the easy plane of magnetization). This anisotropy is not related to the local factors and comes exclusively from the anisotropic exchange interactions involving spins of Ni(II) ions and Kramers doublets of Os(III) centers. In terms of local anisotropy in spin systems, an easy plane of magnetization would correspond to the positive sign of D or conventionally positive anisotropy. It is worth noting that this sign of the global magnetic anisotropy precludes the existence of a barrier for magnetization reversal in the $Ni^{II}_3Os^{III}_2$ cluster. This explains the fact that in contrast with the trigonal bipyramidal $Mn^{III}_2Mn^{II}_3$ cluster that is a SMM,[16] the $Ni^{II}_3Os^{III}_2$ cluster is barrierless and therefore does not exhibit SMM behavior.

Unfortunately, we have not been able to obtain sufficiently large and stable single crystals to perform a detailed experimental study of magnetic anisotropy and corroborate the proposed theoretical approach. The work on the modification of the crystal growth procedure as well as extension of the cluster geometry to the Mn−Os and Cr−Os combinations is currently underway. We expect to provide a more detailed experimental proof of the proposed theoretical model and a systematic study of the new types of Os(III)-containing complexes in the future.

The theoretical treatment in this article was based on the parametric phenomenological Hamiltonian that properly takes into account the symmetry of the system. An actual task is the microscopic evaluation of the exchange parameters. Progress in this area has been recently achieved.[22,23] Although the spin−orbit coupling for Os(III) is strong, the corrections arising from the mixing of excited multiplets can contribute to the pattern of low-lying states. In this view, the recent progress in the use of the symmetry-adapted basis in the evaluation of the exchange systems is to be mentioned.[24] It should be noted that in the limit of strong spin−orbit coupling stabilizing the Kramers doublet in the Os^{III} ion, the Jahn−Teller interaction is reduced.[25,26] Nevertheless the second-order corrections to g factors may affect the anisotropic contributions. We expect to consider these questions elsewhere.

Summary

We have successfully modeled the magnetic properties of the new pentanuclear complex $\{[Ni(tmphen)_2]_3[Os(CN)_6]_2\}\cdot 6CH_3CN$, which is the first magnetic cluster incorporating the $[Os(CN)_6]^{3-}$ anion. It is found that the system can be described by the effective Hamiltonian expressed in terms of a pseudo-spin-1/2 operator related to the ground Kramers doublet of the Os(III) ion and the true spin operators for the Ni(II) ion (s_3 = 1). The system is found to be highly anisotropic with the trigonal Z axis being a hard axis of magnetization. The sign of the magnetic anisotropy, however, precludes the possibility of SMM behavior for this cluster. This conclusion based on the microscopic approach might be helpful in the design of molecular magnets with controlled magnetic anisotropy and a higher barrier for magnetization reversal.

Acknowledgment. B.S.T. and K.R.D. gratefully acknowledge financial support from the USA−Israel Binational Science Foundation (grant no. 2006498). The financial support of the Supreme Council for Science and Technological Development of Moldova is also appreciated. K.R.D. is grateful for partial support of this research by the Department of Energy, the National Science Foundation, and The Welch Foundation.

Appendix

TABLE A1: Bond Distances and Angles Around Os(III) Centers in the Ni_3Os_2 Complexes[a]

atoms	distance (Å)	atoms	angle (deg)
Os(1)−C(1D)	2.06(2)	C(1D)−Os(1)−C(6D)	174.3(7)
Os(1)−C(2D)	2.07(2)	C(1D)−Os(1)−C(2D)	89.7(8)
Os(1)−C(3D)	2.08(2)	C(6D)−Os(1)−C(2D)	90.0(7)
Os(1)−C(4D)	2.08(2)	C(1D)−Os(1)−C(5D)	93.2(7)
Os(1)−C(5D)	2.08(2)	C(6D)−Os(1)−C(5D)	87.1(6)
Os(1)−C(6D)	2.06(2)	C(2D)−Os(1)−C(5D)	177.0(7)
		C(1D)−Os(1)−C(4D)	85.7(6)
Os(2)−C(1E)	2.07(2)	C(6D)−Os(1)−C(4D)	88.5(6)
Os(2)−C(2E)	2.09(2)	C(2D)−Os(1)−C(4D)	90.3(7)
Os(2)−C(3E)	2.08(2)	C(5D)−Os(1)−C(4D)	90.3(6)
Os(2)−C(4E)	2.08(2)	C(1D)−Os(1)−C(3D)	92.7(8)
Os(2)−C(5E)	2.12(2)	C(6D)−Os(1)−C(3D)	93.1(8)
Os(2)−C(6E)	2.08(2)	C(2D)−Os(1)−C(3D)	90.7(9)
		C(5D)−Os(1)−C(3D)	88.7(8)
		C(4D)−Os(1)−C(3D)	178.1(8)
		C(1E)−Os(2)−C(3E)	92.0(6)
		C(1E)−Os(2)−C(4E)	176.6(7)
		C(3E)−Os(2)−C(4E)	88.6(6)
		C(1E)−Os(2)−C(6E)	87.0(6)
		C(3E)−Os(2)−C(6E)	179.0(6)
		C(4E)−Os(2)−C(6E)	92.4(5)
		C(1E)−Os(2)−C(2E)	88.3(7)
		C(3E)−Os(2)−C(2E)	89.6(7)
		C(4E)−Os(2)−C(2E)	95.1(6)
		C(6E)−Os(2)−C(2E)	90.6(6)
		C(1E)−Os(2)−C(5E)	89.5(6)
		C(3E)−Os(2)−C(5E)	92.6(7)
		C(4E)−Os(2)−C(5E)	87.1(6)
		C(6E)−Os(2)−C(5E)	87.1(6)
		C(2E)−Os(2)−C(5E)	176.9(6)

[a] See Figure A1 for the numbering of atoms.

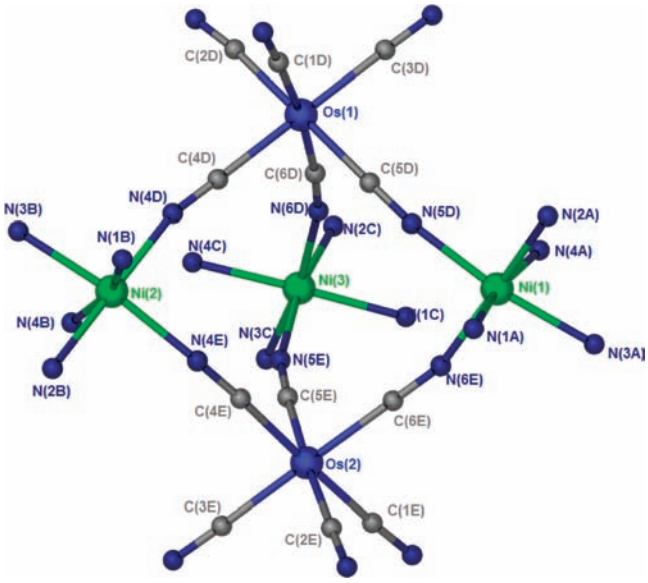

Figure A1. Numbering of atoms in the Ni_3Os_2 complex.

The exchange parameters, $J_{\alpha\beta}(i, j)$, are expressed in terms of the exchange integrals $J_{||}$, $J_{\perp}$, and the angle θ

$$
\begin{aligned}
J_{XX}(1,3) = J_{XX}(2,3) = J_{||}\sin^2(\theta) + \\
J_{\perp}\cos^2(\theta), \quad J_{YY}(1,3) = J_{YY}(2,3) = J_{\perp}, \\
J_{ZZ}(1,3) = J_{ZZ}(1,4) = J_{ZZ}(1,5) = J_{ZZ}(2,3) = J_{ZZ}(2,4) = \\
J_{ZZ}(2,5) = J_{||}\cos^2(\theta) + J_{\perp}\sin^2(\theta), \\
J_{XZ}(1,3) = J_{ZX}(1,3) = -J_{XZ}(2,3) = -J_{ZX}(2,3) \\
= \sin(\theta)\cos(\theta)(J_{||} - J_{\perp}), \\
J_{XY}(1,3) = J_{YX}(1,3) = J_{XY}(2,3) = J_{YX}(2,3) = 0, \\
J_{XX}(1,4) = J_{XX}(1,5) = J_{XX}(2,4) = J_{XX}(2,5) \\
= (1/4)[J_{||}\sin^2(\theta) + J_{\perp}\cos^2(\theta)] + (3/4)J_{\perp}, \\
J_{YY}(1,4) = J_{YY}(1,5) = J_{YY}(2,4) = J_{YY}(2,5) \\
= (3/4)[J_{||}\sin^2(\theta) + J_{\perp}\cos^2(\theta)] + (1/4)J_{\perp}, \\
J_{XZ}(2,4) = J_{ZX}(2,4) = J_{XZ}(2,5) = J_{ZX}(2,5) \\
= -J_{XZ}(1,4) = -J_{ZX}(1,4) = -J_{XZ}(1,5) = -J_{ZX}(1,5) \\
= (1/2)\sin(\theta)\cos(\theta)(J_{||} - J_{\perp}) \\
J_{YZ}(1,5) = J_{ZY}(1,5) = J_{YZ}(2,4) = J_{ZY}(2,4) \\
= -J_{YZ}(1,4) = -J_{ZY}(1,4) = -J_{YZ}(2,5) = -J_{ZY}(2,5) \\
= (\sqrt{3}/2)\sin(\theta)\cos(\theta)(J_{||} - J_{\perp}) \\
J_{XY}(1,4) = J_{YX}(1,4) = \mathrm{J}_{XY}(2,4) = \mathrm{J}_{YX}(2,4) \\
= -J_{XY}(1,5) = -J_{YX}(1,5) = -J_{XY}(2,5) = -J_{YX}(2,5) \\
= (\sqrt{3}/4)\sin^2(\theta)(J_{||} - J_{\perp}) \quad (6)
\end{aligned}
$$

References and Notes

(1) Gatteschi, D.; Sessoli, R. *Angew. Chem., Int. Ed* **2003**, *42*, 268.

(2) Gatteschi, D.; Sessoli, R.; Villain, J. *Molecular Nanomagnets*; Oxford University Press: Oxford, U.K., 2006.

(3) Borrás-Almenar, J. J.; Clemente-Juan, J. M.; Coronado, E.; Palii, A. V.; Tsukerblat, B. S. *J. Phys. Chem. A* **1998**, *102*, 200.

(4) Borras-Almenar, J. J.; Clemente-Juan, J. M.; Coronado, E.; Palii, A. V.; Tsukerblat, B. S. *Chem. Phys.* **2001**, *274*, 131.

(5) Borrás-Almenar, J. J.; Clemente-Juan, J. M.; Coronado, E.; Palii, A. V.; Tsukerblat, B. S. *Chem. Phys.* **2001**, *274*, 145.

(6) Palii, A. V.; Tsukerblat, B. S.; Coronado, E.; Clemente-Juan, J. M.; Borrás-Almenar, J. J. *J. Chem. Phys.* **2003**, *118*, 5566.

(7) Borras-Almenar, J. J.; Clemente-Juan, J. M.; Coronado, E.; Palii, A. V.; Tsukerblat, B. S. *J. Solid State Chem.* **2001**, *159*, 268.

(8) Palii, A. V.; Ostrovsky, S. M.; Klokishner, S. I.; Tsukerblat, B. S.; Berlinguette, C. P.; Dunbar, K. R.; Galán-Mascarós, J. R. *J. Am. Chem. Soc.* **2004**, *126*, 16860.

(9) Tsukerblat, B. S.; Palii, A. V.; Ostrovsky, S. M.; Kunitsky, S. V.; Klokishner, S. I.; Dunbar, K. R. *J. Chem. Theory Comput.* **2005**, *1*, 668.

(10) Mironov, V. S.; Chibotaru, L. F.; Ceulemans, A. *Phys. Rev. B* **2003**, *67*, 014424–1.

(11) Mironov, V. S.; Chibotaru, L. F.; Ceulemans, A. *J. Am. Chem. Soc.* **2003**, *125*, 9750.

(12) Palii, A. V.; Ostrovsky, S. M.; Klokishner, S. I.; Tsukerblat, B. S.; Dunbar, K. R. *Chem. Phys. Chem.* **2006**, *7*, 871.

(13) Palii, A. V.; Ostrovsky, S. M.; Klokishner, S. I.; Tsukerblat, B. S.; Schelter, E. J.; Prosvirin, A. V.; Dunbar, K. R. *Inorg. Chim. Acta* **2007**, *360*, 3915.

(14) Long, J. R. Molecular Cluster Magnets. In *Chemistry of Nanostructured Materials*; Yang, P., Ed.; World Scientific Publishing: Hong Kong, 2003; p 291.

(15) Sokol, J. J.; Hee, A. G.; Long, J. R. *J. Am. Chem. Soc.* **2002**, *124*, 7656.

(16) Berlinguette, C. P.; Vaughn, D.; Cañada-Vilalta, C.; Galán-Mascarós, J.-R.; Dunbar, K. R. *Angew. Chem., Int. Ed.* **2003**, *42*, 1523.

(17) Schelter, E. J.; Prosvirin, A. V.; Reiff, W. M.; Dunbar, K. R. *Angew. Chem., Int. Ed.* **2004**, *43*, 4912.

(18) Hilfiger, M.; Shatruk, M.; Prosvirin, A. *Chem. Commun.* **2008**, 5752.

(19) Albores, P.; Slep, L. D.; Baraldo, L. M.; Baggio, R.; Garland, M. T.; Rentschler, E. *Inorg. Chem.* **2006**, *45*, 2361.

(20) Abraham, A.; Bleaney, B. *Electron Paramagnetic Resonance of Transition Ions*; Dover: New York, 1986.

(21) Mironov, V. S. *Dokl. Phys. Chem.* **2007**, *415*, 199.

(22) Atanasov, M.; Barras, J.-L.; Benco, L.; Daul, C. *J. Am. Chem. Soc.* **2000**, *122*, 4718.

(23) Atanasov, M.; Comba, P.; Daul, C. *Inorg. Chem.* **2008**, *47*, 2449.

(24) Schnalle, R.; Schnack, J. *Phys. Rev. B* **2009**, *79*, 104419.

(25) Bersuker, I. B.; Polinger, V. Z. *Vibronic Interactions in Molecules and Crystals*; Springer-Verlag: Berlin, 1989.

(26) Bersuker, I. B. *The Jahn−Teller Effect*; Cambridge University Press: New York, 2006.

JP902197N